Transactions on Additive Manufacturing Meets Medicine
Trans. AMMM, 2023, Vol. 5, No 1, Article ID 798, 9 Pages

Infinite Science Publishing

Original Research Article

Multilayer microneedle array patches by combining inkjet printing and micromolding – A technical evaluation

L. C. Lammerding[1*], S. Braun[1], and J. Breitkreutz[1]

[1] *Institute of Pharmaceutics and Biopharmaceutics, Heinrich Heine University, Duesseldorf, Germany*
[*] *Corresponding author, email: lukas.lammerding@hhu.de*

Abstract: Microneedle array patches offer the possibility to deliver active pharmaceutical ingredients bypassing the gastrointestinal tract. Dissolvable microneedles pierce the stratum corneum, dissolve under the skin and release the drug to the body. Inkjet printing is known to be a possible manufacturing method for microneedle array patches and a suitable tool for preparing personalized medicine. Multilayer microneedle array patches consist of at least two layers clearly separated from each other. A suitable ink candidate for the production of the first layer of microneedles has been found. The printing process was optimized, and the jetted droplets were analyzed in terms of their velocity and volume. Lisinopril has been used as a model drug with a peptidomimetic structure. Different heights of the drug-containing layer of the microneedles were successfully produced resulting in the possibility to vary the dosage of the microneedle array patches between 11.5 – 34 µg. The production was successful resulting in sharp and intact needle tips and the microneedles did not shrink. The height of the needle tips was precisely adjusted. The produced microneedle array patches showed good mechanical properties and did not break during the simulation of the application procedure. Testing the insertion into an artificial skin membrane model resulted in at least 381 µm insertion depths. Therefore, these multilayer microneedle array patches were promising candidates to enable efficient drug delivery. Inkjet printing could be used as a precise manufacturing method for personalized medicine with varying dosages of microneedle array patches for the patients' needs. Multilayer microneedle array patches are promising candidates for adjusting the dissolution profile of dissolvable microneedles by preparing several layers from various polymers and combining these polymers in one single microneedle array patch. Different drug substances may be combined in a single patch.

I. Introduction

Oral administration of active pharmaceutical ingredients (APIs) remains the most commonly used way for drug delivery. Due to different reasons like poor drug solubility, degradation by the acidic gastric conditions and poor permeation through the intestinal walls, oral drug delivery is limited for some drugs [1]. Especially the oral application of peptides like vaccines or monoclonal antibodies is still challenging. Parenteral drug delivery, e.g., subcutaneous injections, may solve these problems but can result in other problems. Pain during the injection and needle aversion may decrease adherence to parenteral drug delivery [2]. The use of a transdermal drug delivery system (TDDS) has been described to overcome these problems [3]. TDDS reduce peak concentrations and may limit adverse effects [4].

But transdermal drug delivery is limited to a few APIs because of the barrier function of the stratum corneum (SC) which consists of 10 – 15 µm thick layers of corneocytes [5]. TDDS predominantly deliver APIs by passive diffusion. The diffusion rate is highly dependent on the chemical structure of the APIs. Different techniques to increase the penetration and permeation of APIs through the SC have been investigated. For example, enhancers [6] and iontophoresis have been described [7]. Enhancers like various alcohols, oils or fatty acids may damage or irritate the skin when used for a long time period [8]. Iontophoresis increases the permeation rate of some ionic APIs using electric current [9]. Microneedle array patches (MAPs) may be used to overcome these problems. A MAP consists of micrometer-sized (typically in a range between 100 – 1000 µm) needles with the ability to pierce the SC and bypass the barrier function of the skin [10]. An advantage

of the application using microneedles is that their application is painless [11]. Microneedles are too short to reach nerve fibers. This can increase the adherence of patients suffering from needle aversion. Different types of MAPs have been described in literature like (1) solid microneedles [12] consisting of a solid material like glass or metal [13] piercing the SC. After that, an API-containing patch is applied to the punctured skin and the permeation of the API is increased ("patch-and-poke"). Solid microneedles may also be coated with an API-containing film-coating (2) [14]. The coating dissolves after application and enables drug delivery. Other types of MAPs described in literature are (3) separable MAPs [15], (4) swellable microneedles [16], (5) hollow microneedles [17], and (6) biodegradable MAPs [18]. Separable MAPs are inserted into the skin and after application the microneedles are separated from the baseplate and remain in the skin for drug delivery. Swellable microneedles are described to be an interesting possibility for extended release of APIs [19]. Hollow microneedles enable the diffusion through the needles and APIs are usually located in the baseplate of the MAP. It has been described that the manufacturing of biodegradable MAPs is possible using poly(lactic-co-glycolic acid). Dissolvable MAPs (7) had become increasingly important in the last few years [20]. Dissolvable MAPs are usually produced using micromolding techniques where micrometer-sized cavities of a silicon mold are filled with an API-containing polymeric solution. To obtain rapidly dissolving microneedles, water-soluble polymers are used for the production. The cavities are filled by the application of overpressure [21] or centrifugal forces [22]. After drying, the polymer forms the microneedles. Different polymers have been described for the production of dissolvable MAPs like povidone [23], cellulose ethers [24] or various co-polymers [25]. After piercing the SC, the polymer dissolves rapidly under the skin and transdermal drug delivery is induced. Different APIs have already been delivered using MAPs, e.g. various vaccines and peptides like insulin [26]. All types of MAPs have in common that the drug loading is quite limited. Therefore, new methods for the production of MAPs are needed or the application of MAPs is limited to low-dosed and high-effective APIs. Micromolding has a disadvantage in terms of filling the cavities. It is not possible to determine exactly which cavity should be filled with which amount of polymeric solution. Inkjet printing (IJP) has been described to overcome this problem [27]. A precise dosing is feasible using IJP. Pharmaceutical IJP has been described as a useful tool for the preparation of various dosage forms for personalized medicine [28]. In the principle of drop generation, it can be distinguished between drop-on-demand (DoD) and continuous inkjet printing (CIJ) [29]. DoD enables the possibility to apply exactly one droplet per pixel. The droplets usually have a volume between 1 – 100 pl [30] making a precise dosing feasible. Droplets are usually generated using piezo-electric crystals. The application of the voltage deforms the piezoelectric crystal which results in the release of a droplet from the ink reservoir. Even the manufacturing of multilayer MAPs has been described [31] but for the production the micromolding technique has been used only.

The aim of this study was to jet a printable polymeric ink into micrometer-sized cavities of a micro mold made from silicone. First, the most suitable ink settings had to be found by varying the dwell time and determining the resulting droplet momentum (product of droplet velocity and volume/mass). After that, multilayer MAPs have been produced. The first layer has been produced using inkjet printing and contained the API. Povidone was chosen as the polymer to form rapidly dissolving needle tips. Lisinopril was chosen as the model API because of its peptidomimetic structure to simulate the production of MAPs containing peptides. The amount of lisinopril-containing ink jetted into each cavity has been varied between 150, 250 and 450 droplets. The second layer of the MAPs was applied using centrifugation as a micromolding technique. The prepared multilayer MAPs were characterized in terms of their mechanical properties, insertion behavior into an artificial skin model and drug loading.

II. Material and methods

II.I. Material

Polyvinyl pyrrolidone (povidone) of different grades (Kollidon K17 and K30) and amaranth were obtained from BASF (Ludwigshafen, Germany), ethyl cellulose (EC, Aqualon N-10) from Ashland (Düsseldorf, Germany). Glycerol 85 % and polysorbate 20 (Tween 20) were purchased from Caesar & Loretz (Hilden, Germany). Lisinopril dihydrate was ordered from Zhejiang Huahai Pharmaceutical (Zhejiang, China). Triethyl citrate (Citrofol AI) was purchased from Jungbunzlauer (Basel, Switzerland). Ethanol in analytical grade was obtained from an in-house supplier. Sodium dihydrogen phosphate was received from AppliChem (Glenview, Illinois, USA) and phosphoric acid from Sigma Aldrich (St. Louis, Missouri, USA). Acetonitrile in analytical grade was purchased from VWR (Darmstadt, Germany). Demineralized water was used as a solvent and starting material for producing ultra-purified water using a Milli-Q apparatus (Merck, Darmstadt, Germany) for high-performance liquid chromatography (HPLC) analysis. Silicone molds for the production of microneedle array patches (MAPs) were kindly provided by LTS Lohmann-Therapiesysteme (Andernach, Germany). Every mold contained 37 pyramidal-shaped cavities (300 x 300 µm base, 900 µm length, 2 mm interspacing). An exemplary silicon mold is shown in Fig. 1.

Infinite Science Publishing

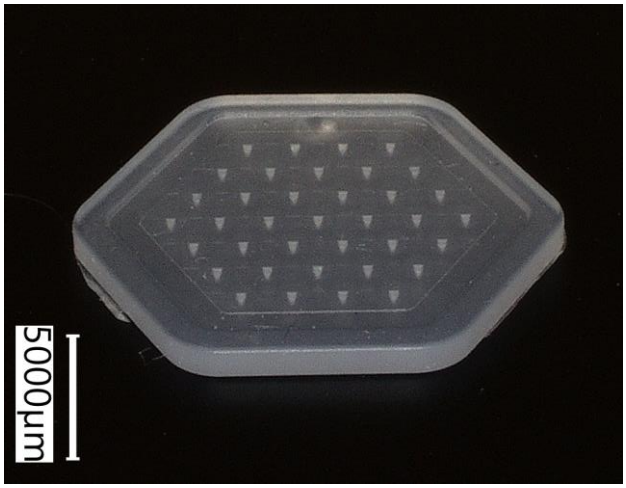

Figure 1: Silicon mold containing 37 pyramidal-shaped cavities

II.II. Methods

II.II.I. Preparation of microneedle array patches

25.0 g povidone K17, 1.0 g polysorbate 20 and 3.0 g glycerol 85 % were dissolved in 71.0 g demineralized water. This mixture (formulation 1) was stirred until a clear solution was obtained and was used for the production of the first layer of the MAPs using inkjet printing. Polysorbate 20 was added to increase the jettability and the wettability. Glycerol 85 % was added as a plasticizer. Lisinopril dihydrate was added until a concentration of 35 mg/ml was reached. Amaranth was added for coloring. After performing inkjet printing the needle tips were dried for two hours in an exsiccator filled with freshly activated silica gel at 27 °C. The second layer consisted of ethyl cellulose and was applied using centrifugation. 20.0 g ethyl cellulose was dissolved in 80.0 g ethanol. 4.0 g triethyl citrate was added as a plasticizer and the mixture was stirred until a clear solution was obtained (formulation 2). 75 µl of this solution was applied to the silicon mold and centrifugation was performed for 20 min at a speed of 3776 g, using the Multifuge 1L (Heraeus, Hanau, Germany). Subsequently, the third layer consisting of povidone K30 was added to the MAPs. For this purpose, 30.0 g povidone K30 was dissolved in 66.5 g demineralized water. 0.5 g polysorbate 20 and 3.0 g glycerol 85 % were added after a clear solution was obtained (formulation 3). 300 µl of formulation 3 have been pipetted on the silicon mold to form a coherent baseplate. Drying was performed for 16 h using the same conditions mentioned before. The formulations for the production of each layer are summarized in Table 1 and the manufacturing process of multilayer dissolvable MAPs in Fig. 2.

Table 1: Compositions of polymer solutions used for the production of multilayer MAPs

Name	Formulation 1	Formulation 2	Formulation 3
Polymer	Povidone K17	Ethyl cellulose	Povidone K30
Surfactant	Polysorbate 20	-	Polysorbate 20
Plasticizer	Glycerol 85 %	Triethyl citrate	Glycerol 85 %
Solvent	Water	Ethanol	Water

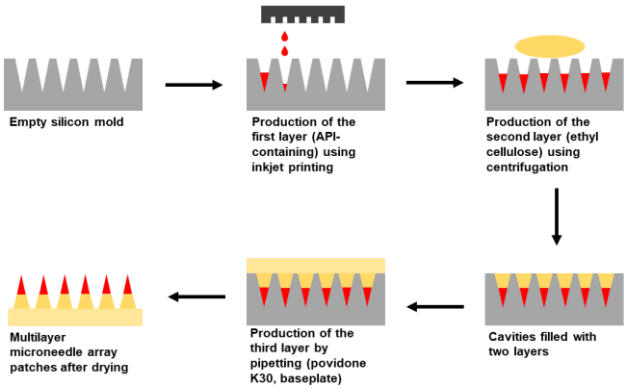

Figure 2: Manufacturing process of multilayer MAPs using inkjet printing and centrifugation

II.II.II. Inkjet printing and influence of the dwell time

Inkjet printing was used to produce the first layer of the MAPs. This layer contained lisinopril and was colored with amaranth to visualize the printing process. Inkjet printing was performed using the desktop inkjet system PixDro LP50 (Meyer Burger, Eindhoven, The Netherlands) equipped with a piezo-driven drop-on-demand printhead (Spectra SL-128 AA, Fujifilm Dimatrix, Santa Clara, CA, USA). The temperature of the printhead was set to 30 °C ensuring constant and comparable conditions during the manufacturing process. A pressure of -18.30 mbar was applied to the ink reservoir. The pulse voltage was set to 100.0 V with a pulse shape of 90 %. Droplets were jetted using a single nozzle.

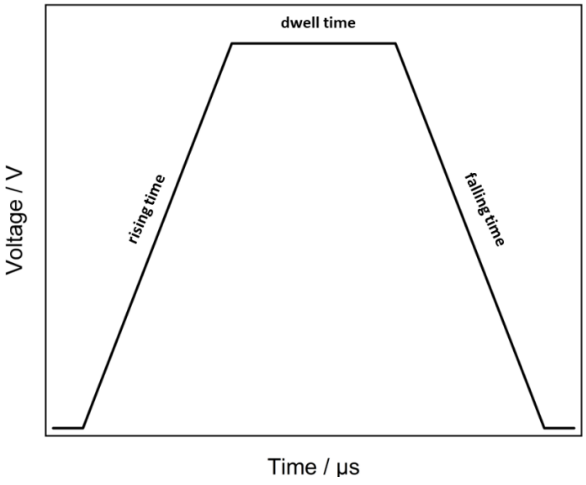

Figure 3: Example actuation waveform applied to the piezo-driven printhead

The actuation waveform applied at the printhead has a big impact on the volume and the speed of the jetted droplets [32]. An example actuation wave is shown in Fig. 3. First, the voltage is constantly rising. When the set maximum voltage is reached, it is held for a certain time (dwell time). After that, the voltage decreases until the initial value is reached.

The dwell time has been varied between 0 – 25 µs to find the most suitable printing settings. Pictures of the droplets were taken using the built-in camera system of the printer. The integrated software tool Advanced Drop Analysis (ADA, V2.4.2) was used to analyze the volumes and velocities of the droplets. The density of the ink has been determined in a previous work [27] and was used to calculate the mass of the droplets. The resulting droplet momentum (DM) was calculated according to equation (1) at each dwell time using the velocity and mass of the droplets. Droplets were jetted using frequencies of 500 and 1000 Hz.

$$DM = v\left(\frac{m}{s}\right) * m(kg) \quad (1)$$

After the most suitable printing settings were found, the first layer of MAPs was produced. MAPs with three different filling heights were manufactured to vary the dosage. Therefore, the number of droplets filled into each cavity was varied between 150, 250 and 450 drops.

II.II.III. Mechanical stability of microneedle array patches

The mechanical stability of the MAPs was investigated using a method described in literature [33]. MAPs were attached needle-downwards to the cylindrical probe of a TA.XTplus texture analyser (Stable Micro Systems, Godalming, UK). The texture analyser was set to compression mode and the probe was moved downwards. The microneedles were pressed against the aluminum block of the texture analyser. The compression force was set to 32 N and has been held for 30 s. It has been described that these are the average application conditions when administering MAPs [33]. Pre- and post-test speeds were set to 1.0 mm/s and the test speed to 0.5 mm/s. The test started when the trigger force of 0.049 N has been reached. The height of the microneedles was determined before and after the compression using digital light microscope VHX7000 (Keyence, Osaka, Japan). The height reduction of the microneedles was calculated according to equation (2):

$$HR = \frac{h\,(before) - h\,(after)}{h\,(before)} * 100\ \% \quad (2)$$

where HR is the percentage height reduction, h (before) is the height of the needles before compression and h (after) after compression. The height reduction has been used for describing the mechanical stability of MAPs. Six single needles were measured. Arithmetic means ($\bar{x}$) and standard deviations (sd) were calculated.

II.II.IV. Insertion in Parafilm

Insertion of MAPs was simulated using Parafilm M sheets (Neenah, Wisconsin, USA) as an artificial skin membrane model. It has been shown and validated that eight layers of Parafilm showed comparable mechanical properties to human skin [33]. MAPs were attached to the moveable probe of the texture analyser like described before. The texture analyser was set to compression mode. Pre- and post-test speeds were set to 1.0 mm/s, and trigger force to 0.049 N. The probe moved downwards, and the microneedles were pressed against eight layers of Parafilm using a test speed of 1.19 mm/s. A force of 32 N has been held for 30 seconds when the trigger force was reached. After that, MAPs were carefully removed from the Parafilm. The holes created in each layer of the Parafilm were counted using the digital microscope Keyence VHX7000. The percentage number of microneedles which pierced each layer was calculated according to equation (3)

$$Holes\ (\%) = \frac{no.\ Holes\ (layer)}{no.\ Holes\ (total)} * 100\% \,. \quad (3)$$

No. Holes (layer) are the holes created in each layer and no. holes (total) are the number of microneedles in a single MAP. All tests were performed in triplicate. Arithmetic means ($\bar{x}$) and standard deviations (sd) were calculated.

II.II.V. Lisinopril assay

The lisinopril content of the prepared MAPs was analyzed using HPLC coupled with UV spectroscopy. An Agilent 1260 infinity (Agilent Technologies, Santa Clara, CA, USA) HPLC system with a diode array UV absorption detector were used. A reversed stationary phase was applied (Knauer Eurosphere II, 100-5 C18A, Berlin, Germany). Identity and quantitation of Lisinopril was investigated using an isocratic method. The mobile phase was sodium dihydrogen phosphate buffer adjusted to ph 3.5 by phosphoric acid 85 % and acetonitrile (80:20). Flowrate was set to 1.0 ml/min and the detection was performed at a wavelength of 210 nm. Injection volume was set to 20 µl and the column temperature to 40 °C. The mean retention time of lisinopril was 2.7 minutes.

The tips of the MAPs were dissolved in 10.0 ml water and the solutions were subjected to the assay. All measurements were performed in triplicate. Arithmetic means ($\bar{x}$) and standard deviations (sd) were calculated.

III. Results and discussion

III.I. Influence of the dwell time

Inkjet printing was performed using the setting mentioned in section II.II.II. The most suitable settings for the jetting process to produce the tips of the microneedles had to be identified first. Investigations were performed to determine the influence of the dwell time and the jetting frequency. The dwell time was varied between 0 and 25 µs at 0.5 µs steps. These variations were applied for frequencies of 500 and 1000 Hz. Pictures of the jetted droplets were taken and the resulting droplet momenta (see equation (1)) were calculated. The results are shown in Fig. 4.

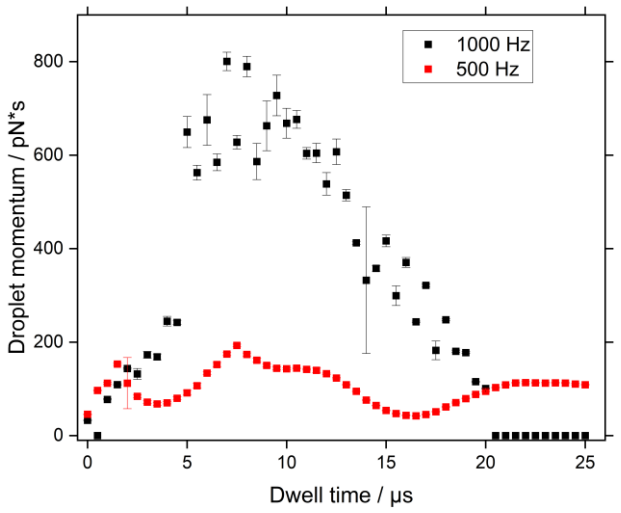

Figure 4: Influence of the dwell time on the droplet momentum; investigations were performed at frequencies of 500 and 1000 Hz using the PixDro LP50 inkjet printer equipped with the piezo-driven printhead Spectra SL-128AA (nozzle diameter: 50 µm); n=9, $\bar{x}$ ± sd

The DM is higher when jetting has been performed at the higher frequency of 1000 Hz. The droplets were bigger and had a higher velocity. It was previously described that the DM (equation 1) should be as high as possible to enable a faster printing process. If the droplets are larger, fewer droplets are needed to fill the cavities. This can shorten the printing process and the overall production time of MAPs. The velocities of the droplets should be fast, too. A higher jetting speed results in a more precise printing pattern. The DM decreased when jetting was performed using increased dwell times of 20 – 25 µs. DM dropped to 0 pN*s when jetting was performed with a frequency of 1000 Hz and dwell times of more than 20.5 µs. The maximum DM was reached at dwell times of 7.0 µs (1000 Hz) or 7.5 µs (500 Hz). The resulting DMs were 800.46 ± 19.77 pN*s (1000 Hz) and 192.94 ± 2.62 pN*s. The dwell time was set to 7.0 µs and the frequency to 1000 Hz for our manufacturing method of the first layer of multilayer MAPs. It was not possible to perform inkjet printing at higher frequencies because the jetting time would be too short to completely fill the cavities and successfully control the process.

The resulting droplets had a mean volume of approx. 60 pl. Three different filling heights for the first layer were produced. 150, 250 and 450 drops were jetted into each cavity of the silicon mold.

III.II. Visualization of produced MAPs

The produced MAPs were investigated using the digital light microscope. Images of the entire MAPs were taken as well as images of single needles. An exemplary dissolvable multilayer MAP with 37 needle tips is shown in Fig. 5.

Filling the cavities of the silicon mold using ink jetting was feasible and precisely adjusted. The height of the colored layer was comparable for all needles. The height of the colored first layer was investigated as well as the height of three single microneedles. The results for the heights of both measurements are shown in Table 2.

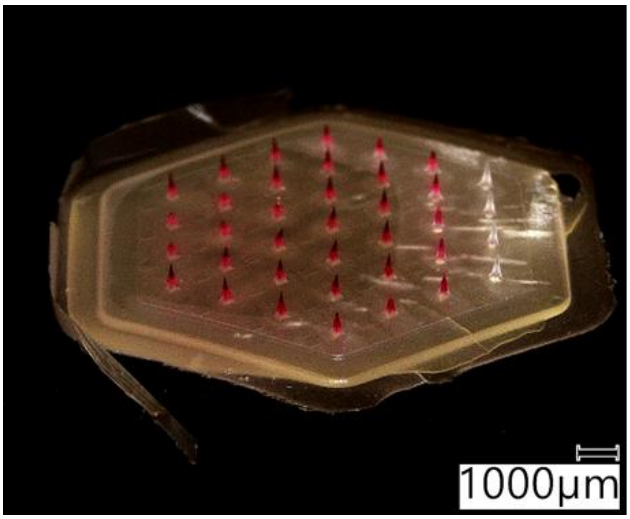

Figure 5: Digital microscopic image of multilayer microneedle array patch; zoom: 10x

Table 2: Needle heights of the first, API-containing layer and the entire microneedles; n=3, $\bar{x}$ ± sd

Name	Height of first layer / µm	Height of entire needles / µm
150 drops	425.04 ± 9.39	901.31 ± 6.61
250 drops	653.38 ± 6.11	902.71 ± 1.20
450 drops	901.83 ± 3.26	901.83 ± 3.26

All microneedles were of pyramidal shape and had sharp tips. It was demonstrated that inkjet printing is a method to successfully fill micrometer-sized cavities for the production of microneedles. The height of the first layer was successfully varied by jetting different numbers of droplets per cavity. The filling height of the first layer was 425.04 ± 9.39 µm (150 drops) and 653.38 ± 6.11 µm (250 drops). The different layers are clearly separated (Fig. 5). A single cavity had a total volume of 27 nl. Jetting was repeated with a droplet volume of approx. 60 pl. Therefore, the entire cavity was filled when 450 drops were jetted. In this case, no clear separation between the layers was observed.

Even the baseplate was colored red because of the diffusion of amaranth. Fig. 6 shows exemplary MAPs and the measurements of single microneedles produced by jetting different numbers of droplets in every cavity. The data suggest that ink jetting is a very precise option to vary filling heights and therefore the dosage of multilayer MAPs. The total filling height could be adjusted to three different heights.

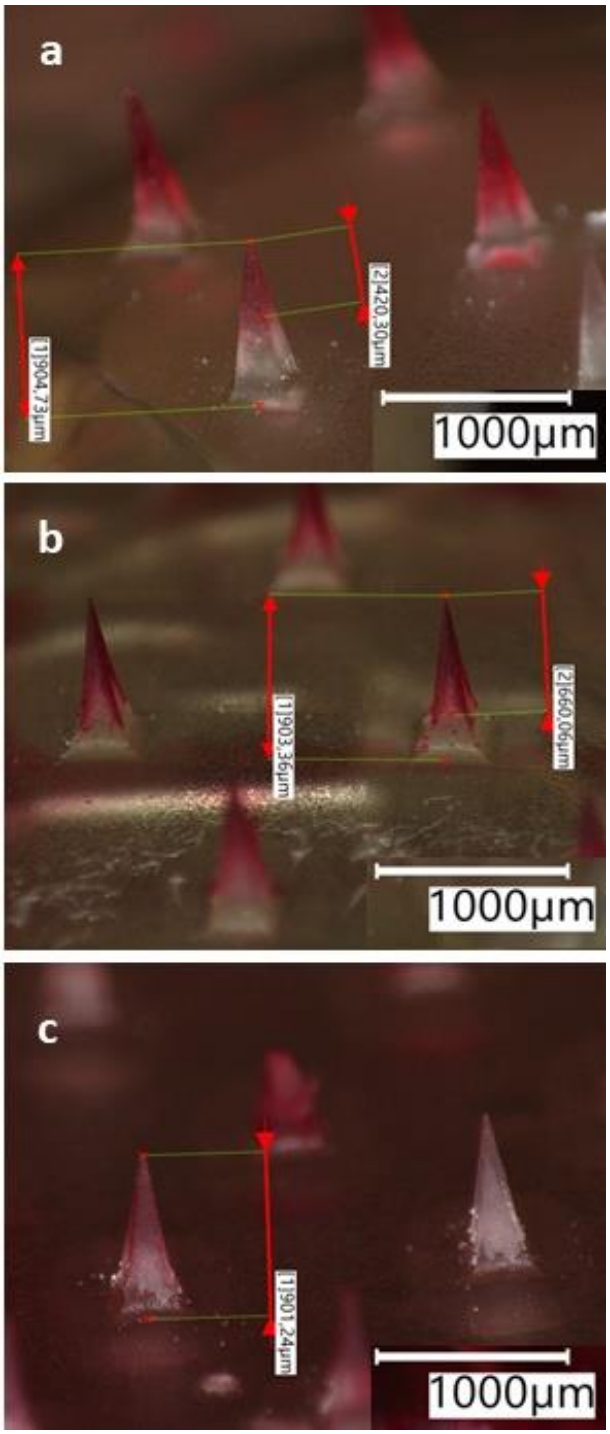

Figure 6: Multilayer microneedles produced by jetting 150 drops (A), 250 drops (B) and 450 drops (C) per cavity; measurements of the API-containing layer and of whole needles; zoom: 50x

Standard deviations were quite small indicating that the manufacturing process is precise and reproducible. It can be assumed that a variation in the filling height of the first layer leads to a precise variation in the dose strength. That could be an interesting approach to combine different polymers and/or APIs in a single MAP. The variation of a matrix polymer could lead to MAPs showing different dissolution behaviors and could be a possibility to modify the drug release.

III.III. Mechanical strength of MAPs

The results of investigating the mechanical stability of dissolvable multilayer MAPs are shown in Fig. 7.

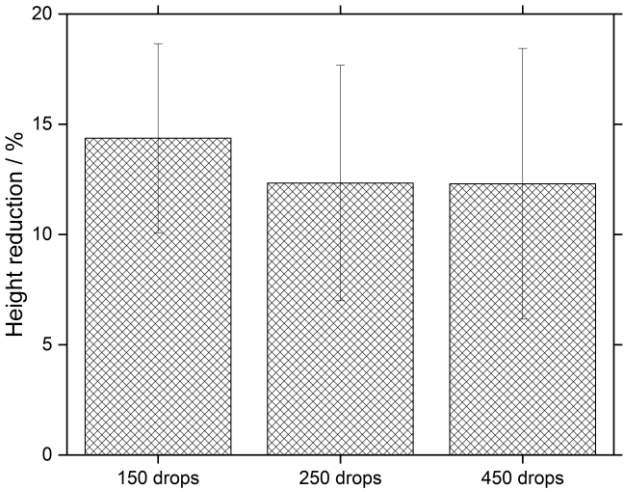

Figure 7: Mechanical stability of MAPs described as height reduction; n=6, $\bar{x}$ ± sd

The height reduction of MAPs after compression was comparable and independent of the height of the first layer (14.36 ± 4.29 % for 150 drops, 12.33 ± 5.34 % for 250 drops and 12.30 ± 6.14 % for 450 drops). It has been described that a height reduction of 10 – 15 % results in microneedles suitable for an efficient drug delivery [34]. Microneedles must not break during compression. That results in failing this test because it could be expected that these needles would break during application. Povidone K17 used for the manufacturing process of the first layer is known as a brittle polymer. Therefore, glycerol 85 % was added in a certain concentration to the formulation as a plasticizer. The addition of too much plasticizer would result in soft MAPs. Soft MAPs would have a significantly higher height reduction and are potentially too soft to pierce the skin and could not achieve transdermal drug delivery. All tested microneedles remained sharp and intact after the mechanical stability testing. No breaking of the needles was observed (see Fig. 8). Overall, the produced multilayer MAPs showed sufficient mechanical stability without breaking when a force of 32 N was applied. This force is the average force applied to a MAP by patients during the administration procedure [33]. Therefore, dissolvable multilayer MAPs should be mechanically strong enough for real-life application.

Infinite Science Publishing

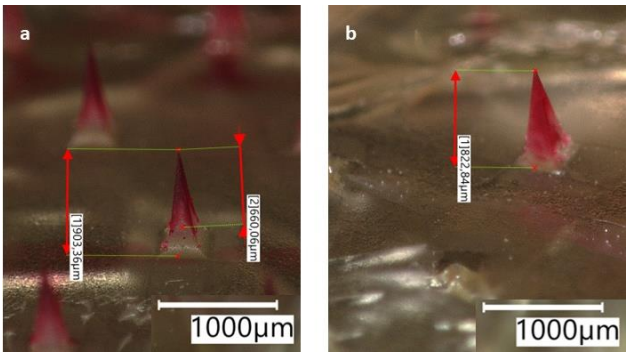

Figure 8: Exemplary microneedles before (a, height of approx. 903 µm) and after (b, height of approx. 823 µm) compression

III.IV. Insertion in Parafilm

Parafilm M was used as an artificial skin membrane to simulate the insertion of dissolvable multilayer MAPs as described by Larraneta [33]. The results are shown in Fig. 9.

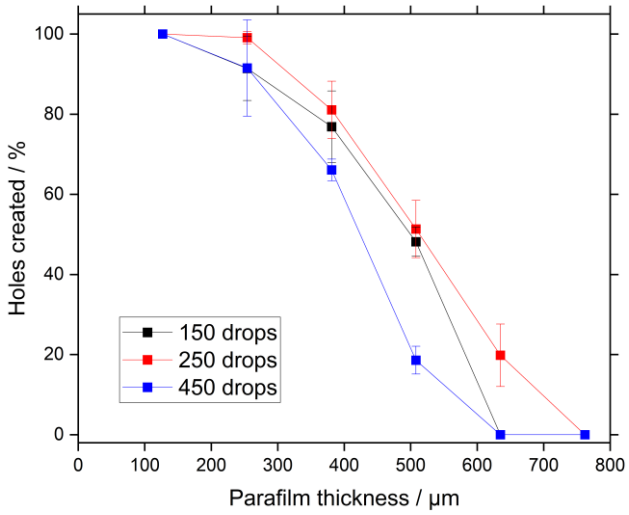

Figure 9: Insertion of dissolvable multilayer MAPs into Parafilm as an artificial skin membrane model; n=3, $\bar{x}$ ± sd; thickness of every Parafilm layer was 127 µm

Most of the microneedles (91.40 ± 7.99 % for 150 drops, 99.10 ± 1.56 % for 250 drops and 91.52 % for 450 drops) pierced at least two layers of Parafilm which is equal to 254 µm penetration depth. Each layer of Parafilm has a thickness of 127 µm. It has been described that at least two layers must be punctured to provide sufficient and efficient drug delivery [35]. Therefore, it should be possible to administer APIs transdermally using the produced dissolvable multilayer MAPs. It could be expected that these microneedles insert in even deeper layers of the skin. 76.89 ± 8.92 % of the microneedles pierced the third layer of Parafilm (equal to 381 µm) when the API-containing needle tip has been produced by jetting 150 drops per cavity. The results are comparable to the needles the API-containing layer was produced by jetting 250 and 450 drops per cavity, respectively. 81.08 ± 7.15 % (250 drops) and 66.09 ± 2.71 % (450 drops) pierced the third layer of Parafilm (equal to 381 µm). The insertion into deeper layers of the microneedles in which the first API-containing layer was made by jetting 450 drops showed different results than the microneedles in which fewer drops were used to produce the first layer. Only 18.60 ± 3.47 % of these needles pierced the fourth layer of Parafilm (equal to 508 µm) compared to 48.18 ± 3.66 % (150 drops) and 51.35 ± 7.15 % (250 drops). An explanation may be that povidone is a brittle polymer resulting in less stable microneedles. All produced MAPs showed sufficient insertion in at least two layers (equal to 254 µm) using Parafilm as a skin model. Further investigations should show whether transdermal drug delivery is feasible and whether different skin layers can be targeted and adjusted by the different heights of the layers containing the API.

III.V. Content determination

Content determination of lisinopril dihydrate after dissolving the needle tips in 10.0 ml demineralized water had been performed using an HPLC assay. The jetted droplets had a volume of approx. 60 pl. The target content of lisinopril filled into an entire MAP was calculated according to equation (4)

$$m(API) = V(droplet) * n * 37 * c \qquad (4)$$

where V(droplet) is the volume of a single droplet, n is the number of droplets jetted per cavity, 37 is the number of all cavities in a MAP and c is the concentration of the ink used for the printing process (35 mg/ml). The calculated target values are shown in Table 3 as well as the mass of lisinopril found in the MAPs. 99.33 ± 5.09 % (150 drops), 103.83 ± 11.55 % (250 drops) and 97.20 ± 0.48 % (450 drops) lisinopril were recovered. That indicated that the printing process was precise and the dosage could be varied between 11.58 and 33.99 µg in 8 µg steps. Inkjet printing is a good possibility to produce dissolvable multilayer MAPs and to modify the drug loading. Therefore, the production of MAPs using inkjet printing to produce at least one layer of the microneedles was identified to be an interesting idea to manufacture individualized MAPs. The dosage could be varied and customized for the individual needs of a patient.

Table 3: Lisinopril target content and analyzed content in the MAPs; n=3, $\bar{x}$ ± sd

Name	Target content / µg	Content / µg	Content / %
150 drops	11.66	11.58 ± 0.59	99.33 ± 5.09
250 drops	19.43	20.17 ± 2.24	103.83 ± 11.55
450 drops	34.97	33.99 ± 0.17	97.20 ± 0.48

IV. Conclusions

A suitable ink candidate for the manufacturing process of multilayer MAPs has been found. The printing settings were optimized to shorten the production process. It was possible to produce multilayer MAPs using a combination of inkjet printing and centrifugation. A clear separation between all layers was visible. Three different filling

heights of the first layer were successfully produced resulting in the possibility to vary the dosage of the MAPs between 11.58 – 33.99 µg lisinopril per patch. Variations of the dosing were feasible jetting different amounts of droplets into the cavities. Therefore, the production of multilayer MAPs by inkjet printing is an interesting approach to producing MAPs for individualized therapy. The dosage can be varied in small steps between 11.58 and 33.99 µg for the patient's needs. Personalized medicine could be interesting for APIs with a narrow therapeutic index, e.g. cytostatics or hormones. MAPs are often investigated to deliver peptides or vaccines transdermally. Lisinopril was chosen as a peptidomimetic model API. Further investigations using peptides of higher molecular weight would be interesting in order to dose peptides precisely without damaging the tertiary molecular structure. Multilayer MAPs could be an interesting possibility to combine different APIs in one MAP. The polymer matrix of both layers could be varied to obtain MAPs with the desired dissolution profile. All produced MAPs showed good mechanical properties and insertion in an artificial skin membrane model. Further investigations should show whether an insertion in human skin is feasible. Permeation studies are needed as well to get more information about a possible application. Overall, manufacturing multilayer MAPs using inkjet printing is a novel technique and could enrich the knowledge and opportunities producing MAPs. Combining inkjet printing and micromolding could combine the advantages of both manufacturing techniques. A precise dosing of highly potent APIs can be achieved using inkjet printing. Micromolding can fasten the manufacturing process. However, the production of MAPs by inkjet printing is limited to povidone as a polymer. Finding other polymers suitable for the printing process is another challenge.

Acknowledgments

The authors would like to thank LTS Lohmann Therapie-Systeme for kindly providing the silicon molds for the production of microneedle array patches. The authors would like to thank Dr. Tobias Auel and Lee Roy Oldfield (Heinrich Heine University Duesseldorf) for preparing sample holders by fused deposition modeling (3D printing) to dry the microneedle array patches.

Author's statement

The authors state no conflict of interest. Informed consent has been obtained from all individuals included in this study.

References

[1] M. R. Prausnitz, S. Mitragotri, and R. Langer, "Current status and future potential of transdermal drug delivery," *Nat Rev Drug Discov*, vol. 3, no. 2, pp. 115-24, Feb 2004, doi: 10.1038/nrd1304.

[2] H. S. Gill and M. R. Prausnitz, "Does needle size matter?," *J Diabetes Sci Technol*, vol. 1, no. 5, pp. 725-9, Sep 2007, doi: 10.1177/193229680700100517.

[3] J. W. Wiechers, "The barrier function of the skin in relation to percutaneous absorption of drugs," *Pharm Weekbl Sci*, vol. 11, no. 6, pp. 185-98, Dec 15 1989, doi: 10.1007/BF01959410.

[4] Y. Gao *et al.*, "Highly porous silk fibroin scaffold packed in PEGDA/sucrose microneedles for controllable transdermal drug delivery," *Biomacromolecules*, vol. 20, no. 3, pp. 1334-1345, Mar 11 2019, doi: 10.1021/acs.biomac.8b01715.

[5] R. J. Scheuplein and I. H. Blank, "Permeability of the skin," *Physiol Rev*, vol. 51, no. 4, pp. 702-47, Oct 1971, doi: 10.1152/physrev.1971.51.4.702.

[6] K. A. Walters and J. Hadgraft, *Pharmaceutical skin penetration enhancement*. Informa Health Care, 1993.

[7] S. Khamoushian *et al.*, "Transdermal delivery of insulin using combination of iontophoresis and deep eutectic solvents as chemical penetration enhancers: In vitro and in vivo evaluations," *J Pharm Sci*, Mar 14 2023, doi: 10.1016/j.xphs.2023.03.005.

[8] U. T. Lashmar, J. Hadgraft, and N. Thomas, "Topical application of penetration enhancers to the skin of nude mice: a histopathological study," *J Pharm Pharmacol*, vol. 41, no. 2, pp. 118-22, Feb 1989, doi: 10.1111/j.2042-7158.1989.tb06405.x.

[9] Y. Zhou *et al.*, "An integrated Mg battery-powered iontophoresis patch for efficient and controllable transdermal drug delivery," *Nat Commun*, vol. 14, no. 1, p. 297, Jan 18 2023, doi: 10.1038/s41467-023-35990-7.

[10] S. Henry, D. V. McAllister, M. G. Allen, and M. R. Prausnitz, "Microfabricated microneedles: a novel approach to transdermal drug delivery," *J Pharm Sci*, vol. 87, no. 8, pp. 922-5, Aug 1998, doi: 10.1021/js980042+.

[11] S. Kaushik *et al.*, "Lack of pain associated with microfabricated microneedles," *Anesthesia & Analgesia*, vol. 92, no. 2, pp. 502-504, 2001, doi: 10.1213/00000539-200102000-00041.

[12] F. J. Verbaan *et al.*, "Assembled microneedle arrays enhance the transport of compounds varying over a large range of molecular weight across human dermatomed skin," *J Control Release*, vol. 117, no. 2, pp. 238-45, Feb 12 2007, doi: 10.1016/j.jconrel.2006.11.009.

[13] W. Martanto, S. P. Davis, N. R. Holiday, J. Wang, H. S. Gill, and M. R. Prausnitz, "Transdermal delivery of insulin using microneedles in vivo," *Pharm Res*, vol. 21, no. 6, pp. 947-52, Jun 2004, doi: 10.1023/b:pham.0000029282.44140.2e.

[14] E. Moreno *et al.*, "Skin vaccination using microneedles coated with a plasmid DNA cocktail encoding nucleosomal histones of Leishmania spp," *Int J Pharm*, vol. 533, no. 1, pp. 236-244, Nov 25 2017, doi: 10.1016/j.ijpharm.2017.09.055.

[15] L. Y. Chu and M. R. Prausnitz, "Separable arrowhead microneedles," *J Control Release*, vol. 149, no. 3, pp. 242-9, Feb 10 2011, doi: 10.1016/j.jconrel.2010.10.033.

[16] M. C. Kearney, E. Caffarel-Salvador, S. J. Fallows, H. O. McCarthy, and R. F. Donnelly, "Microneedle-mediated delivery of donepezil: Potential for improved treatment options in Alzheimer's disease," *Eur J Pharm Biopharm*, vol. 103, pp. 43-50, Jun 2016, doi: 10.1016/j.ejpb.2016.03.026.

[17] P. M. Wang, M. Cornwell, J. Hill, and M. R. Prausnitz, "Precise microinjection into skin using hollow microneedles," *J Invest Dermatol*, vol. 126, no. 5, pp. 1080-7, May 2006, doi: 10.1038/sj.jid.5700150.

[18] M. He, G. Yang, X. Zhao, S. Zhang, and Y. Gao, "Intradermal implantable PLGA microneedles for etonogestrel sustained release," *J Pharm Sci*, vol. 109, no. 6, pp. 1958-1966, Jun 2020, doi: 10.1016/j.xphs.2020.02.009.

[19] G. Yang, M. He, S. Zhang, M. Wu, and Y. Gao, "An acryl resin-based swellable microneedles for controlled release intradermal delivery of granisetron," *Drug Dev Ind Pharm*, vol. 44, no. 5, pp. 808-816, May 2018, doi: 10.1080/03639045.2017.1414230.

[20] N. W. Kang *et al.*, "Microneedles for drug delivery: recent advances in materials and geometry for preclinical and clinical studies," *Expert Opin Drug Deliv*, vol. 18, no. 7, pp. 929-947, Jul 2021, doi: 10.1080/17425247.2021.1828860.

[21] S. Rojekar *et al.*, "Etravirine-loaded dissolving microneedle arrays for long-acting delivery," *Eur J Pharm Biopharm*, vol. 165, pp. 41-51, Aug 2021, doi: 10.1016/j.ejpb.2021.04.024.

[22] M. Champeau, D. Jary, L. Mortier, S. Mordon, and S. Vignoud, "A facile fabrication of dissolving microneedles containing 5-aminolevulinic acid," *Int J Pharm*, vol. 586, 119554, Aug 30 2020, doi: 10.1016/j.ijpharm.2020.119554.

[23] A. Panda, A. Shettar, P. K. Sharma, M. A. Repka, and S. N. Murthy, "Development of lysozyme loaded microneedles for dermal applications," *Int J Pharm*, vol. 593, p. 120104, Jan 25 2021, doi: 10.1016/j.ijpharm.2020.120104.

[24] N. N. Aung, T. Ngawhirunpat, T. Rojanarata, P. Patrojanasophon, P. Opanasopit, and B. Pamornpathomkul, "HPMC/PVP dissolving microneedles: a promising delivery platform to promote trans-epidermal delivery of alpha-arbutin for skin lightening," *AAPS PharmSciTech*, vol. 21, no. 1, p. 25, Dec 17 2019, doi: 10.1208/s12249-019-1599-1.

[25] A. Carcamo-Martinez *et al.*, "Enhancing intradermal delivery of tofacitinib citrate: Comparison between powder-loaded hollow microneedle arrays and dissolving microneedle arrays," *Int J Pharm*, vol. 593, 120152, Jan 25 2021, doi: 10.1016/j.ijpharm.2020.120152.

[26] M. H. Ling and M. C. Chen, "Dissolving polymer microneedle patches for rapid and efficient transdermal delivery of insulin to diabetic rats," *Acta Biomater*, vol. 9, no. 11, pp. 8952-61, Nov 2013, doi: 10.1016/j.actbio.2013.06.029.

[27] L. C. Lammerding and J. Breitkreutz, "Technical evaluation of precisely manufacturing customized microneedle array patches via inkjet drug printing," *Int J Pharm*, p. 123173, Jun 25 2023, doi: 10.1016/j.ijpharm.2023.123173.

[28] Y. Thabet, D. Lunter, and J. Breitkreutz, "Continuous inkjet printing of enalapril maleate onto orodispersible film formulations," *Int J Pharm*, vol. 546, no. 1-2, pp. 180-187, Jul 30 2018, doi: 10.1016/j.ijpharm.2018.04.064.

[29] G. D. Martin, S. D. Hoath, and I. M. Hutchings, "Inkjet printing - the physics of manipulating liquid jets and drops," *Journal of Physics: Conference Series*, vol. 105, 2008, doi: 10.1088/1742-6596/105/1/012001.

[30] B. Derby, "Inkjet printing of functional and structural materials: Fluid property requirements, feature stability, and resolution," *Annual Review of Materials Research*, vol. 40, no. 1, pp. 395-414, 2010, doi: 10.1146/annurev-matsci-070909-104502.

[31] M. Li, L. K. Vora, K. Peng, and R. F. Donnelly, "Trilayer microneedle array assisted transdermal and intradermal delivery of dexamethasone," *Int J Pharm*, vol. 612, p. 121295, Jan 25 2022, doi: 10.1016/j.ijpharm.2021.121295.

[32] A. B. Aqeel, M. Mohasan, P. Lv, Y. Yang, and H. Duan, "Effects of the actuation waveform on the drop size reduction in drop-on-demand inkjet printing," *Acta Mechanica Sinica*, vol. 36, no. 5, pp. 983-989, 2020, doi: 10.1007/s10409-020-00991-y.

[33] E. Larraneta *et al.*, "A proposed model membrane and test method for microneedle insertion studies," *Int J Pharm*, vol. 472, no. 1-2, pp. 65-73, Sep 10 2014, doi: 10.1016/j.ijpharm.2014.05.042.

[34] A. D. Permana *et al.*, "Selective delivery of silver nanoparticles for improved treatment of biofilm skin infection using bacteria-responsive microparticles loaded into dissolving microneedles," *Mater Sci Eng C Mater Biol Appl*, vol. 120, p. 111786, Jan 2021, doi: 10.1016/j.msec.2020.111786.

[35] F. Volpe-Zanutto *et al.*, "Artemether and lumefantrine dissolving microneedle patches with improved pharmacokinetic performance and antimalarial efficacy in mice infected with Plasmodium yoelii," *J Control Release*, vol. 333, 298-315, May 10 2021, doi: 10.1016/j.jconrel.2021.03.036.